Molecular dynamics of the interfacial properties of partially fluorinated polymer dispersed liquid crystal gratings

2008 J. Phys. D: Appl. Phys. 41 235302

(http://iopscience.iop.org/0022-3727/41/23/235302)

IOP PUBLISHING JOURNAL OF PHYSICS D: APPLIED PHYSICS

J. Phys. D: Appl. Phys. **41** (2008) 235302 (10pp) doi:10.1088/0022-3727/41/23/235302

Molecular dynamics of the interfacial properties of partially fluorinated polymer dispersed liquid crystal gratings

Zhigang Zheng[1,2], **Ji Ma**[3], **Yonggang Liu**[1] **and Li Xuan**[1,4]

[1] State Key Laboratory of Applied Optics, Changchun Institute of Optics, Fine Mechanics and Physics, Chinese Academy of Sciences, Changchun, 130033, People's Republic of China
[2] Graduate School of Chinese Academy of Sciences, Beijing, 100039, People's Republic of China
[3] Liquid Crystal Institute, Kent State University, Kent, OH 44240, USA

E-mail: zhigang1982@sina.com

Received 1 July 2008, in final form 29 September 2008
Published 4 November 2008
Online at stacks.iop.org/JPhysD/41/235302

Abstract

The interfacial properties of polymer dispersed liquid crystal (PDLC) gratings influenced by partial matrix fluorination are studied through molecular dynamics methods. The miscibility between the fluorine-substituted monomer and other materials in the prepolymer mixture is evaluated by using the solubility parameters of molecules. The interfacial effect of different fluorination levels is analysed theoretically. The results indicate that most fluorine-substituted monomers are distributed on the interface between the monomer and the LC. The interaction energy on the interface decreases with increasing fluorination, which can improve the electro-optical tunable performance of such gratings. However, it should also be noted that excessive fluorination may lead to penetration of fluorine-substituted monomers into the LC medium. Such a result will block the normal diffusion of LC during the photo-initiated polymerization-induced phase separation process. Through calculation of the radial distribution function, a reasonable alignment structure for LCs near the interface is given. The calculation of the order parameter shows that fluorination causes disorder of their orientation.

(Some figures in this article are in colour only in the electronic version)

1. Introduction

Polymer dispersed liquid crystal (PDLC) gratings are a very promising kind of electro-optical device. Because of its electric field switchability, sub-millisecond response and simple fabrication, this type of grating can be applied in optical communications, integrated optics, optical data storage and flat panel displays [1–4]. The ingenious conception of an electrically-tunable grating recorded through holography in a PDLC film was originally proposed by Sutherland *et al* in 1993 [5]. The prepolymer syrup, which is a mixture of photosensitive monomers and nematic liquid crystals (LCs), is exposed under an interference field. After exposure, an alternating LC-rich and polymer-rich lamella structure is formed due to photopolymerization of the monomers and diffusion of the LCs in a photo-initiated polymerization-induced phase separation (PIPS) process [5–9]. Because of the electric field response of LC molecules and the refractive index modulation between LC-rich and polymer-rich lamella, the diffraction efficiency can be switched. Unlike the conventional PDLC devices, the LC droplets in PDLC grating are very small, typically less than 50–200 nm [6, 7, 10, 11], so the light scattering of PDLC grating is very weak throughout the near UV to IR spectrum and better optical properties are obtained.

However, the intricate physical-chemistry mechanisms during PIPS block the normal diffusion of LC, and lead to an incomplete phase separation. As a result, a blurred phase separation interface is formed, which not only distorts the optical properties of the grating but also leads to very poor interfacial properties (large interface energy and surface tension). The poor interface consequently gives rise to a very high threshold voltage and bad electro-optical properties. Some researchers consider that good interfacial

[4] Author to whom any correspondence should be addressed.

properties are the key issues in improving performance. They select many kinds of surfactant monomers to promote phase separation [12–17], and experimental results show that interfacial properties are indeed improved by these materials. An effective example is a fluorine-substituted monomer which, due to its highly electronegative character, has a low surface free-energy. On the other hand, the fluorine atoms enhance the oleophobic properties of the monomer and promote the phase separation. Schulte *et al* and Sarkar *et al* have studied the electro-optical performance and interfacial properties of PDLCs and PDLC gratings by partial matrix fluorination [14–17]. Their results proved that fluorination can lower the interface tension and promote phase separation, thereby increasing the dimension of the LC-rich phase and decreasing the threshold voltage of the device. These results are very helpful. However, because of the restriction of experimental instruments and observation methods, many vital microscopic details of the effect of fluorination on the interfacial properties cannot be resolved directly by experiments. Thus, theoretical analysis is necessary, not only because of the importance of fluorination in these gratings but also because of the tremendous value of theoretical studies in our understanding and prediction of the properties induced by fluorination.

In this paper molecular dynamics (MD) methods are used to investigate the influence of partial fluorination on the interfacial properties. The solubility parameters and diffusion constants of various materials are calculated and compared with each other quantitatively to explain the miscibility and diffusion characteristics of the prepolymer. The molecular interaction energies and the distribution of fluorine-substituted monomers near the interface are investigated through MD simulation. Some results show good agreement with the previous reports. The radial distribution function (RDF) is applied to investigate the root of interaction decrease caused by fluorination, as well as to analyse the LC alignment structure near the interface. The LC orientation is also investigated through calculation of the order parameter. MD may help us to understand the fundamental mechanisms of the improvements in interface properties and phase separation by fluorination. It also provides a guideline when selecting suitable materials for fabricating PDLC gratings.

2. Simulation methodology and theory

2.1. Simulation methodology

All calculations for a polymer–liquid crystalline composite system are carried out using the complete atomistic model. Before the MD calculation, a suitable force field should be assigned to every atom in the molecule to make them move during MD calculation. This step is very important and determines the correctness of the calculation. In our work, the polymer consistent force field (PCFF) [18, 19] is selected. This is an extension of the consistent force field, CFF [20–22], and is always applied to simulate polymers and organic materials such as LCs or any of the monomers mentioned above. Moreover, the PCFF includes many kinds of intra-molecular and intermolecular energies, which makes it very suitable for energy calculations. The force field can be derived from the following expression, where E_{pot} represents the potential energy of the molecule.

$$
\begin{aligned}
E_{\text{pot}} = {} & \sum_{b} [K_2(b-b_0)^2 + K_3(b-b_0)^3 + K_4(b-b_0)^4] && (1)\\
& + \sum_{\theta} [H_2(\theta-\theta_0)^2 + H_3(\theta-\theta_0)^3 + H_4(\theta-\theta_0)^4] && (2)\\
& + \sum_{\phi} \{V_1[1-\cos(\phi-\phi_1^0)] + V_2[1-\cos(2\phi-\phi_2^0)] \\
& + V_3[1-\cos(3\phi-\phi_3^0)]\} && (3)\\
& + \sum_{\chi} K_\chi \chi^2 + \sum_{b}\sum_{b'} F_{bb'}(b-b_0)(b'-b_0') && (4)\ (5)\\
& + \sum_{\theta}\sum_{\theta'} F_{\theta\theta'}(\theta-\theta_0)(\theta'-\theta_0') && (6)\\
& + \sum_{b}\sum_{\theta} F_{b\theta}(b-b_0)(\theta-\theta_0) && (7)\\
& + \sum_{b}\sum_{\phi}(b-b_0)[V_1\cos\phi + V_2\cos 2\phi + V_3\cos 3\phi] && (8)\\
& + \sum_{b'}\sum_{\phi}(b'-b_0')[V_1\cos\phi + V_2\cos 2\phi + V_3\cos 3\phi] && (9)\\
& + \sum_{\theta}\sum_{\phi}(\theta-\theta_0)[V_1\cos\phi + V_2\cos 2\phi + V_3\cos 3\phi] && (10)\\
& + \sum_{\phi}\sum_{\theta}\sum_{\theta'} K_{\phi\theta\theta'}\cos\phi(\theta-\theta_0)(\theta'-\theta_0') && (11)\\
& + \sum_{i>j}\frac{q_i q_j}{\varepsilon r_{ij}} + \sum_{i>j}\left[\frac{A_{ij}}{r_{ij}^9} - \frac{B_{ij}}{r_{ij}^6}\right] && (1)\\
& && (12)\ (13)
\end{aligned}
$$

In equation (1), the quartic polynomials of terms 1 and 2 denote bond stretching and angle bending, respectively, which represent the potential energies caused by distortions of bond length and bond angle. Here b_0 is the equilibrium bond length between two atoms, θ_0 is the equilibrium bond angle between two bonds and K_i and H_i ($i = 2, 3, 4$) are ith-order bond stretching parameter and angle bending parameter, respectively. Term 3 is a three-order Fourier expansion for the potential energy caused by torsion between two planes (such as the benzene plane) in the molecules and V_i is the ith-order expansion coefficient ($i = 1, 2, 3$). The out-of-plane bending angles are expressed in term 4, which has been defined in many other publications [20–23], where χ are the out-of-plane internal coordinates and K_χ is the out-of-plane bending

parameter. Terms 5 to 11 are cross-coupling terms of the bond–bond, angle–angle, bond–angle, bond–torsion, angle–torsion and angle–angle–torsion. Here $F_{bb'}$, $F_{\theta\theta'}$, $F_{b\theta}$ and $K_{\varphi\theta\theta'}$ are coupling coefficients, as defined in a prior report [24]. Maple *et al* have shown that these cross-coupling terms make the calculated results more realistic [25]. Coulomb interaction is represented by the electrostatic interaction based on the point charge approximation (term 12) and the van der Waals interaction which is expressed as a 9–6 Lennard-Jones function form (term 13). Terms 12 and 13 are called non-bond action terms, with ε being the vacuum dielectric constant, and A_{ij} and B_{ij} the van der Waals parameters. The parametrization of all coefficients contained in equation (1) can be completed by least-squares fitting to *ab initio* data calculated through the Hartree–Fock approximation, or to data obtained through a great number of experiments. Detailed presentations have been reported by Hwang *et al* and Sun *et al* [20–22].

To investigate the properties of materials it is necessary to build some bulk system before simulation. First, some molecules are put in a cubic box. The volume ($L \times L \times L$) of the box is determined by the material density and the number of molecules it contains. To simulate real macroscopic material systems which contain Avogadro's number of molecules, periodic boundary conditions and periodic mirror images are always used [19]. The two algorithms can be expressed simply as follows. A cubic original box is generated. Simultaneously, many similar virtual boxes are generated and laid around the original one. The number of atoms and their distributions in the virtual boxes are the same as in the original. In the MD simulation, we only need to simulate the original box because the dynamics in the virtual ones are considered to be the same. However, the interactions can be calculated with the virtual boxes under the definition of the cut-off radius. By means of the two algorithms the macroscopic materials can be simulated. Some insightful demonstrations of the periodic boundary conditions and periodic mirror images can be found in many references [19, 26, 37]. In addition, it is worth explaining the cut-off radius: to simplify the calculation a radius (r_c) is set, such that by definition the potential between two atoms is equal to zero when their distance is r_c or larger [19, 37]. The interaction is very small near r_c. Normally, r_c should be a little smaller than half of the dimension, $r_c \leqslant L/2$ [19, 27, 28]. In our simulation, the cut-off radius is chosen to be 9.1 Å.

The PDLC gratings are generally fabricated with the following materials: penta-functional dipentaerythritol hydroxyl pentaacrylate (DPHPA), di-functional neopentyl glycol diacrylate (NPGDA) and nematic LC 5CB (the director of 5CB molecule is defined to be the biphenyl segments). To improve the interfacial properties at the LC/polymer interface, fluorination is necessary. In our simulation, 12-fluorine-substituted dodecafluoroheptyl methacrylate (Actyflon) is used. The chemical structures and corresponding molecular models of the materials are given in figure 1. Before the MD simulations three amorphous boxes (DPHPA, NPGDA, Actyflon) are generated first. Then 25 DPHPA molecules are assembled in a cubic box of dimension 26.65 Å corresponding to a density of 1.155 g cm^{-3} at 298 K. Also, 25 NPGDA molecules, 25 Actyflon molecules are assembled in cubic boxes of sizes 20.32 Å and 21.86 Å, corresponding to densities of 1.054 g cm^{-3} and 1.589 g cm^{-3}, respectively, at 298 K. The densities of the three materials are obtained from Aldrich and XEOGIA Fluorine–Silicon Chemical Company. The 25 5CB molecules are assembled in a 21.65 Å-dimensional box (corresponding to the experimentally tested density 1.020 g cm^{-3} [29]) to generate a nematic phase. The pretilt angle is set to be 0° in the simulation.

To carry out MD calculations at a certain temperature, the energies of the four systems have to be minimized (after this step the systems stay in the most stable state corresponding to 0 K). The minimization is performed by a conjugated gradient method based on the Polak–Ribiere algorithm [30]. The convergence of the calculation is set to be 10^{-5} kcal mol^{-1}. Then thermo-relaxation of the systems at 298 K is carried out under the NVT canonical ensemble (defined as the ensemble under conditions of constant volume V and temperature T in the whole MD process) to equilibrate the systems. In NVT thermo-relaxation, a rescaling velocity coefficient is defined to rescale the value of the velocity of atoms [31–33]. The rescaling makes the system's kinetic energy invariable in the whole calculation, so the system temperature remains invariable. The thermo-statistic algorithm is Anderson's method [34]. The equilibration is carried out for 100 ps with a time step of 1 fs, followed by a data collection period of 50 ps for analysis.

In the PIPS process, the phase separation of the grating plays a decisive role in the interface structure, which is closely related to the optical and electro-optical performance of the grating. To analyse the interfacial properties and investigate the influences of different fluorinated levels, an interface model should be built. First, two amorphous boxes are generated by the method mentioned above. One is a nematic 5CB box, the other is a monomer box. We use the mixture of DPHPA and NPGDA to represent the monomer box, into which 6 DPHPA and 16 NPGDA molecules are put (corresponding to a weight ratio of 1 : 1, as used in all our experiments reported previously [35]), and the density of the system is set to be approximately the average value of DPHPA and NPGDA. Secondly, the two boxes are stacked together to form a bi-layer structure, simulating the interface of LCs and monomers. The fluorination is then simulated by inserting some Actyflon monomers into the interface, to form the monomers/Actyflon/LC tri-layer structure. As shown in figure 2, the dimensions of X and Y are both 18.55 Å, while the thickness (Z direction) of the layer is 22 Å.

Through the two steps mentioned above, four kinds of monomer/Actyflon/LC tri-layers with different fluorinated levels are simulated, cases A, B, C and D corresponding to the insertion of 5, 10, 15 and 20 Actyflon molecules into the interface, respectively. The fluorinated level is enhanced step by step from cases A to D. The simulations indicate that the fluorinated level depends strongly on the numerical density of fluorine. The minimization and thermo-relaxation methodologies and settings are the same as those mentioned above. After MD simulation of the four tri-layers, some effects of fluorination on the interfacial properties, such as interface energy and Actyflon distribution near the interface, can be

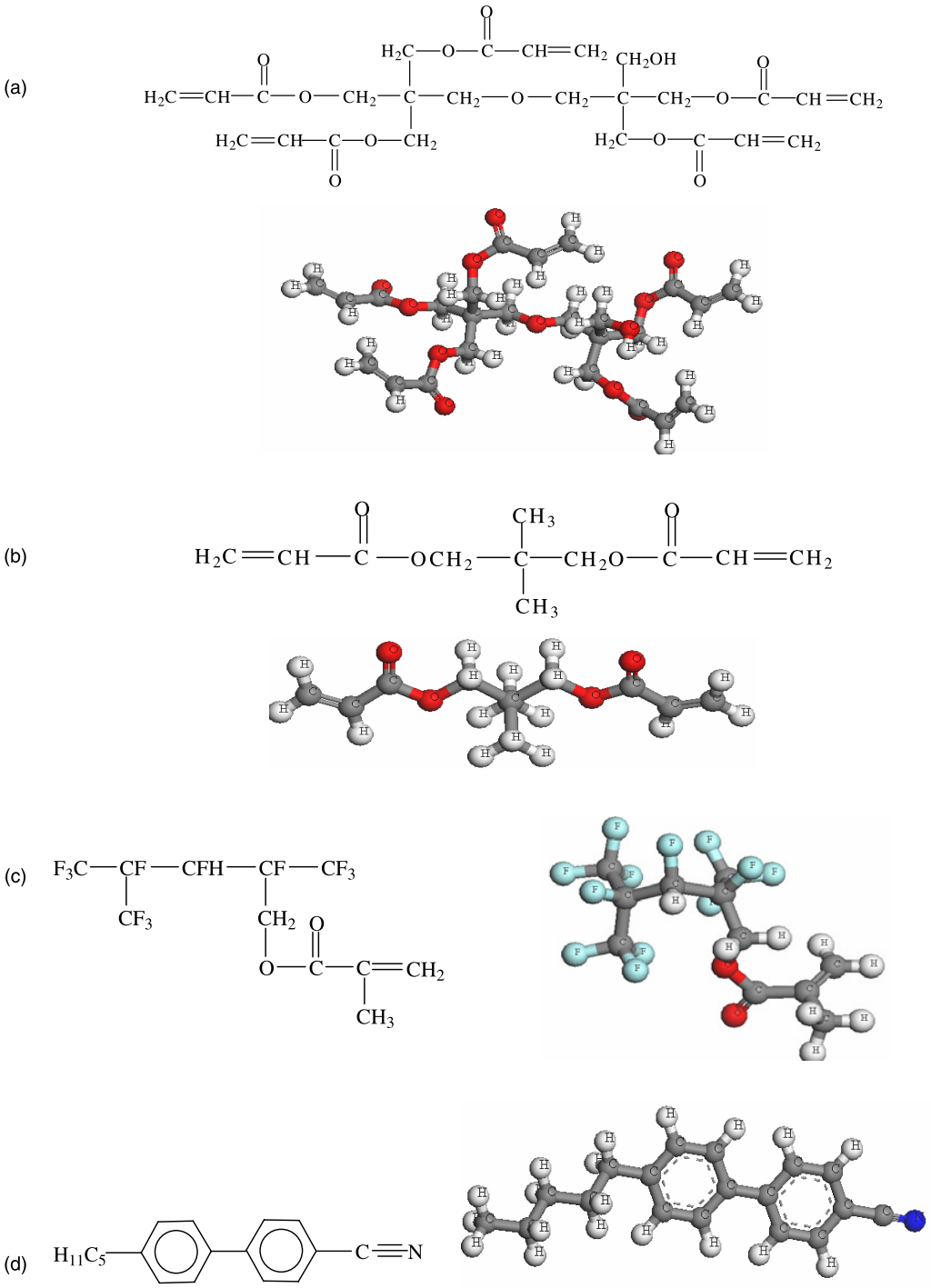

Figure 1. Chemical structure and molecular model of DPHPA (*a*), NPGDA (*b*), Actyflon (*c*) and 5CB (*d*).

analysed. The algorithm to generate the layer structure and other algorithms referred to above are well known to many researchers and details can be found in many publications [19, 36–39], so they will not be discussed here.

2.2. *Theories for calculation and analysis*

2.2.1. Solubility parameter. The miscibility between two kinds of materials can be estimated by the solubility parameter δ of the molecules, which is normally expressed as the square root of the cohesive energy density [40, 42],

$$\delta = E_c^{1/2}. \tag{2}$$

The cohesive energy density E_c is defined as the energy required to break all intermolecular links in a unit volume of the materials [40, 41], and is expressed as

$$E_c = \frac{\Delta H - RT}{V}, \tag{3}$$

where ΔH is the enthalpy change when all intermolecular links are broken (i.e. heat of vaporization) and can be calculated by

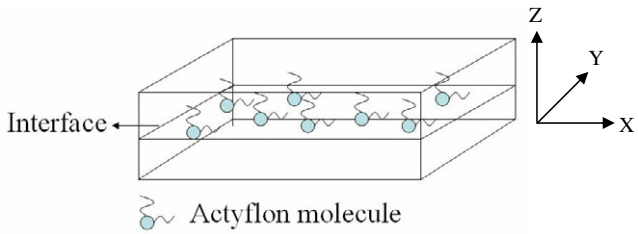

Figure 2. Scheme of monomers/Actyflon/LCs tri-layer structure. Actyflon/LC interface has been shown.

the non-bond terms in equation (1). As usual, R, V and T are the universal gas constant, volume and absolute temperature on the Kelvin scale, respectively.

Substituting equation (3) into equation (2), we can obtain the solubility parameter of one material.

2.2.2. Diffusion constant. The diffusion characteristic of molecules is always investigated through the molecular diffusion constant (D). In MD simulations, the commonest way to calculate this constant is through the mean square displacement (MSD) of every atom in the molecules, from which D can be calculated according to Einstein's diffusion law [19, 37, 38]:

$$\mathrm{MSD} = \sum_{i=1}^{N} \langle |\vec{r}_i(t) - \vec{r}_i(0)|^2 \rangle \tag{4}$$

$$D = \frac{1}{6N} \lim_{t\to\infty} \frac{\mathrm{d}}{\mathrm{d}t}(\mathrm{MSD}), \tag{5}$$

where N in equations (4) and (5) is the number of atoms in the system and equation (5) is the mathematical expression of Einstein's diffusion law.

In our simulation the atoms are moved according to Newton's law under a special force field. At the beginning of the calculation, the original coordinates ($r(0)$) of every atom are saved in the computer. When the MD is started, the position coordinates ($r(t)$) of these atoms are changed with time. Thus, the MSD of atom i at time t can be expressed as $|\vec{r}_i(t) - \vec{r}_i(0)|^2$. Using equation (4), the MSD ensemble average of a system at arbitrary time t can be obtained. From equation (5) it can be found that the slope of the line of the MSD versus time is equal to six times the diffusion constant when the relaxation time $t = \infty$ (that is, to make sure the system reaches equilibrium). Actually, it is impossible and unnecessary to take infinite time to relax the system, because it reaches approximate equilibrium in some tens of picoseconds. We should thus calculate the MSD value at every unit of time, and fit these points as a line. Then we extrapolate the line to $t = \infty$, and the diffusion constant can be obtained by calculating the slope of this line.

2.2.3. Distribution of fluorine atom near the interface. The distribution of fluorine atoms near the interface cannot be observed or measured through experimental methods. However, using MD simulation, this phenomenon can be explained clearly. In this work, the concentration profile of the fluorine atoms is calculated through their position coordinate information and is used to analyse their interpenetration near the interface. This calculation is very important for investigating the dynamical behaviour of fluorine-substituted monomers under different fluorination levels.

2.2.4. Interface energy. In our simulations the interface energy can be calculated through the layer structure model. Assuming that the interface energy is represented as E_{int}; the total energy of the monomer/Actyflon/LC system is E_0; the energy of the LC layer is E_{LC}; the total energy of the monomer/Actyflon bi-layer is E_{M}, thus the interface energy satisfies the expression [43],

$$E_{\mathrm{int}} = E_0 - (E_{\mathrm{LC}} + E_{\mathrm{M}}) \tag{6}$$

from which E_0, E_{LC} and E_{M} can be calculated according to the PCFF expression (equation (1)).

2.2.5. Radial distribution function on the interface. We define an atom on the interface and call it the reference atom. Another atom near the interface is called the target atom. The number of target atoms in the range of r to $r + \Delta r$ from the geometric centre of the reference atom is ΔN, and r should be larger than the radius of the reference atom. The RDF $g(r)$ is then defined as [19],

$$g(r) = \frac{\Delta N}{\rho 4\pi r^2 \Delta r}, \tag{7}$$

where ΔN is the number of atoms in the range of r to $r + \Delta r$ and ρ is the average numerical density of the system. It is easy to find that the number of target atoms in the range is proportional to the value of $g(r)$. The value of ΔN can be calculated through the position coordinates of the atom in the equilibrium state.

In our simulation a fluorine atom (F) on the interface is defined as the reference atom. The target atom is defined as the nitrogen atom (N) contained in the 5CB molecule. Thus the RDF of N near the interface is calculated through the MD program.

2.2.6. Order parameter of LCs near the interface. The orientation behaviour of LCs near the interface is a very important aspect to demonstrate whether the interfacial anchoring to the LC is strong or weak. A more uniform alignment usually corresponds to a stronger anchoring on the interface. Theoretically, the orientation of LC (i.e. order parameter) on the interface is frequently expressed in terms of second-order Legendre polynomials. Thus, the order parameter $S(d)$ is expressed as a function of d, the distance between the midpoints of any two directors [44, 45];

$$S(d) = 0.5[3\cos^2\langle\theta_{ij}(d)\rangle - 1], \tag{8}$$

where $\langle\theta_{ij}\rangle$ is the average angle between two directors i and j.

Table 1. Solubility parameters of various materials (*a*), and the differences between them (*b*).

(*a*)	Materials	DPHPA	NPGDA	Actyflon	N-5CB
	δ (J cm^{-3})$^{0.5}$	17.33	17.34	13.33	18.93
(*b*)	$\Delta\delta$ (J cm^{-3})$^{0.5}$	DPHPA	NPGDA	Actyflon	N-5CB
	DPHPA	0	0.01	4.00	1.60
	NPGDA	0.01	0	4.01	1.59
	Actyflon	4.00	4.01	0	5.60
	N-5CB	1.60	1.59	5.60	0

3. Simulation results and discussions

In the PDLC gratings one of the most important points is the PIPS, which greatly influences the structure of the grating, the LC/polymer interface, the optical performance and the drive properties. The phase separation is decided by many characteristics of the materials, such as the miscibility, diffusion, interface interaction, and so on. Partial fluorination will obviously change some of the material characteristics, so some simulations have been carried out on these aspects. The data collected during the equilibration period (mentioned in section 2) are utilized to analyse the characteristics of fluorine-substituted monomers and the effects of partial fluorination on the interfacial properties.

3.1. Miscibility

The solubility parameters δ of DPHPA, NPGDA, Actyflon and nematic 5CB (N-5CB) are calculated using equations (2) and (3). The results are given in table 1(*a*) and their differences ($\Delta\delta$) are shown in table 1(*b*). The miscibility between two materials can be estimated through the difference in their solubility parameters. If the difference is too large, their miscibility characteristic is poor and vice versa.

From table 1(*a*), δ of Actyflon is 13.33, which is the lowest among the materials used in our system. According to table 1(*b*), the values of $\Delta\delta$ for Actyflon compared with DPHPA, NPGDA and N-5CB are 4.00, 4.01 and 5.60, respectively. This indicates that the miscibility between Actyflon and the other materials is not good. We can deduce from this result that a considerable part of the Actyflon molecules is distributed between the monomers and LCs, which weakens the miscibility between them. Consequently, the phase separation of LCs is promoted during exposure. Jung *et al* have also reported that a large $\Delta\delta$ can lead to a large contact angle between monomers and LCs [42], which implies a smaller surface tension of the interface. This is good for the phase separation process.

3.2. Diffusion characteristics

The diffusion constants of the substances are calculated using the MSD versus time plots (shown in figure 3). Combined with equation (5), the diffusion constants are given in table 2. It can be seen that they are of the same order of magnitude 10^{-8} for NPGDA, Actyflon and N-5CB. For N-5CB this is the same as that derived from experimental results obtained by infrared spectroscopy [46]. Although the LC sample in that experiment was E7, the main composition of E7 is 5CB, about 51% [6], so it is believed that the diffusion constant of N-5CB is on the order of 10^{-8}. Our calculation shows a better agreement with the experimental data.

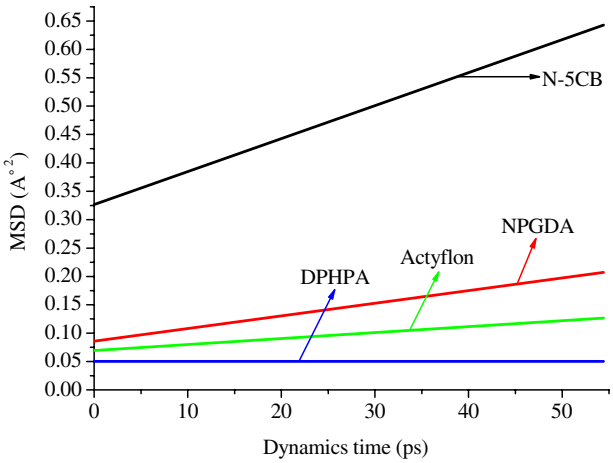

Figure 3. Fitted curves of the MSD versus time for DPHPA, NPGDA, Actyflon and N-5CB.

Table 2. Diffusion constants calculated through Einstein's diffusion law.

Materials	DPHPA	NPGDA	Actyflon	N-5CB
D (cm^2 s^{-1})	7.8×10^{-11}	3.7×10^{-8}	2.0×10^{-8}	8.9×10^{-8}

The calculated diffusion constant of DPHPA is 7.8×10^{-11} cm^2 s^{-1}, which is three orders of magnitude smaller than the other monomers and LCs. Thus DPHPA decreases the diffusion rate of monomers. With regard to other aspects, DPHPA also increases the photopolymerization rate because of its high functionality. According to the theoretical model of Veltri *et al* [47], the higher polymerization rate and slower diffusion rate in the system may lead to a grating with very small LC droplets and a very blurred phase separation interface. The required drive voltage would thus be higher.

However, the two drawbacks of DPHPA can be overcome by fluorination. As shown in table 2, the diffusion constant of Actyflon is almost the same as that of NPGDA and LCs, and is much larger than that of DPHPA. So, on the one hand, adding Actyflon monomer into the prepolymer mixture can increase the diffusion of monomers from the dynamical point of view; on the other hand, such a mono-functional monomer is effective in decreasing the photopolymerization rate. Thus, the polymerization and diffusion of monomers and LCs may reach an equilibration, which would be very beneficial for a better phase separation [7, 51]. As Veltri's model shows, slower photopolymerization enables monomers to diffuse across the grating fringes before they react, and form the so-called POLICRYPS structure with a perfect phase separation interface. Caputo *et al* also reported their experimental results about POLICRYPS [48, 49]. We believe that partial fluorination is another possible way to form this kind of grating, and the results of some ongoing experimental investigations will be reported in the near future.

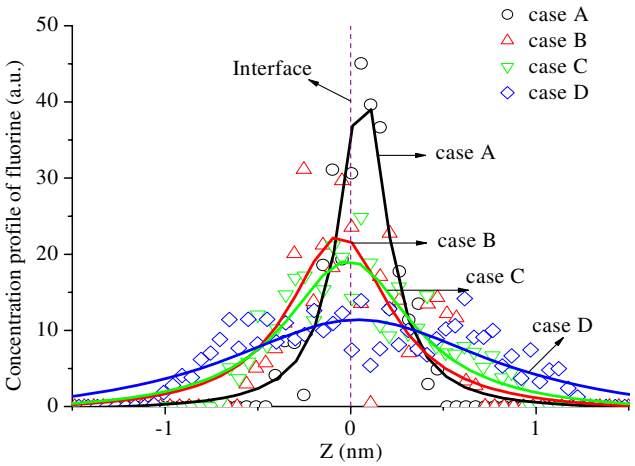

Figure 4. Distribution of fluorine atoms in the cases of A, B, C and D. The discrete points are fitted as Gaussian functions (solid lines).

3.3. Distribution of Actyflon molecules near the interface

It has been demonstrated that the Actyflon may spread out on the interface. To determine the distribution at different fluorination levels, the concentration profile of fluorine atoms near the interface is calculated.

Fluorine distributions for four cases, A, B, C and D (mentioned in section 2), are calculated. The results are shown in figure 4. The abscissa Z of the figure has been defined in figure 2, and the position of the interface is at $Z = 0$. Many discrete points can be found in figure 4. Usually, the concentration near the interface satisfies a Gaussian distribution, so these points are fitted as Gaussian functions. The fitted results for the cases of A, B, C and D are shown in the figure as solid lines. It is clear that, when the number of Actyflon molecules is small (i.e. weak fluorination), such as in case A, the concentration of fluorine atoms on the interface is at its highest (about 40 a.u.). As the fluorination level increases, the concentration decreases gradually to about 10 a.u. (case D).

In addition, it is found that the full width at half maximum (FWHM) of the concentration profile increases rapidly, from 0.25 nm in case A to 1.25 nm in case D. This result indicates that the penetration of Actyflon increases due to growth of the fluorination level. The reasons for this may be twofold. First, the concentration difference of Actyflon on both sides of the interface increases with an increase in the fluorination level. According to Fick's diffusion law [52], the diffusion becomes quite drastic when the concentration difference is large. The other reason may be due to the large diffusion constant of Actyflon, which makes it easier for the molecules to diffuse into the mixture. Consequently, it should be noted that high fluorination of materials may lead to penetration of fluorine-substituted monomers into the LC phase, thus blocking the normal diffusion of LC molecules from the light to the dark strip.

3.4. Interface energy

To investigate the changes in the interfacial anchoring properties under different fluorination levels, the interface energies of cases A, B, C and D are calculated according to equation (6). The results are shown in table 3. The minus sign for E_{int} in the first row indicates a stable interface between Actyflon and LCs since $E_0 < E_{\text{LC}}+E_{\text{M}}$. The absolute values in the second row reflect the strength of the interface interaction.

Comparing the energies in the cases of A to D, we see that the interface energy decreases step by step as the fluorination is increased. The decrease in interface energy is beneficial for the formation of a clear-cut grating structure. Schulte *et al* added two kinds of fluorine-substituted monomers in the prepolymer to fabricate the grating, and found that the phase separation is enhanced, while the anchoring energy to the LCs is decreased [14, 15]. Such results are in good accord with our analysis shown in table 3. It can also be seen that the energy decreases very quickly from case A to C, while there is no significant change from case C to D. The reason for this may be related to the distribution of the Actyflon molecules. As mentioned above, when the number of fluorine-substituted monomers increases on the interface, some of them may penetrate into the LC medium so there is no effective improvement for the interface. Song *et al* have also observed this phenomenon in their experiments [53].

In addition, it should be noted that the fluorinated-monomer/LC interface forms the fluorinated-polymer/LC interface after PIPS; however, their variations of interface energy exhibit the same trends. The reason can be understood according to Patnaik's explanation [50] which had pointed out that the main interacting units in the polymer are also present in the monomer. Although there may be some discrepancies in the energies between the polymer/LC interface and monomer/LC interface, their variation under different fluorination levels is similar. We can therefore assume that the interface energy between the LC and the polymer zones is weakened with the enhancement of fluorination. The decrease in interface energy can lead directly to a decrease in threshold voltage of the devices. Thus, increasing the fluorine content in the prepolymer can decrease the threshold voltage of the grating. Similar results have been noted by Sarkar *et al* and Song *et al* in their investigations [16, 53].

3.5. RDF analysis of 5CB near the fluorinated interface

In the calculation of section 3.4, the interfacial energy decreases with the enhancement of fluorination. To demonstrate this further, the RDF of 5CB near the interface is investigated. Due to the very complex chemical structure of the 5CB molecule, we only calculate the RDF of the nitrogen atom to simplify the calculation. Such a simplification is reasonable because there are no nitrogen atoms on the interface, and each 5CB molecule contains only one nitrogen atom so the RDF can be reflected accurately through the results of nitrogen-RDF. In addition, it is more convenient to study the LC alignment structure under this assumption. The reference atom is defined as the fluorine atom on the interface.

The nitrogen-RDFs near the interface in the four cases A to D are given in figure 5. The abscissa of figure 5 is the distance from the interface to the nitrogen atoms, and the position at $r = 0$ represents the interface. The figure shows that when

Table 3. Interface energies in different fluorinated levels.

Cases[a]	A	B	C	D
E_{int}[b] (kcal mol^{-1})	-110.96 ± 10.21	-76.46 ± 8.63	-41.86 ± 6.09	-45.69 ± 5.81
$\lvert E_{\text{int}}\rvert$[c] (kcal mol^{-1})	110.96 ± 10.21	76.46 ± 8.63	41.86 ± 6.09	45.69 ± 5.81

[a] Cases A, B, C and D correspond to 5, 10, 15 and 20 Actyflon molecules on the interface, respectively.
[b] Minus indicates a stable interface between Actyflon and LCs since $E_0 < E_{\text{LC}} + E_{\text{M}}$.
[c] The absolute values reflect the strength of the interface interaction.

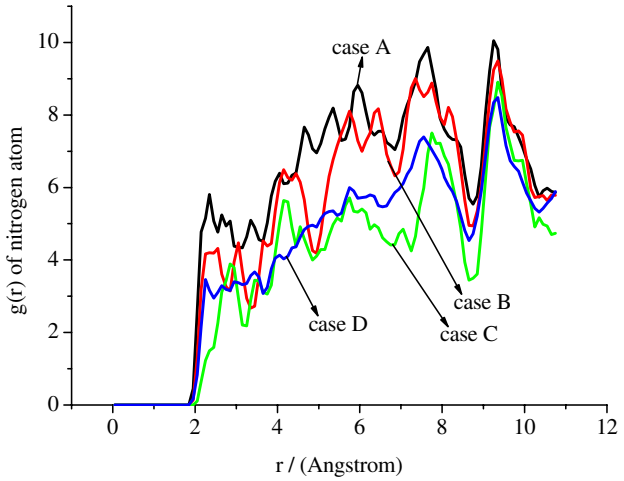

Figure 5. Nitrogen-RDF in the cases of A, B, C and D.

$r \leqslant 2$ Å the value of the nitrogen-RDF in the four cases is 0. It can thus be concluded that the shortest interaction distance between the fluorine atom and the 5CB molecule is larger than 2 Å, which is only about half the width of the benzene ring.

From section 2.2.5, we recall that the number of nitrogen atoms at a certain distance r is proportional to the RDF value at r. According to figure 5, the total number of nitrogen atoms near the interface (from $r = 0$ to $r = 12$ Å) is proportional to the area integral of the RDF curve. Thus, it is evident that the value of the area integral in case A is the largest, becoming smaller and smaller from case A to D (as the fluorination level increases). This result indicates that more 5CB molecules are close to the interface when the fluorination is weak, so in this case the average interaction distance between 5CB and the interface is smaller, and the non-bond energy (i.e. interface energy, terms 12 and 13 in equation (1)) is larger. However, when the fluorination is greater, the distance (r_{ij} in equation (1)) between 5CB and the interface is increased so the non-bond energy becomes smaller. The conclusions agree well with our analysis from the interface energy point of view.

In addition, it can be found from figure 5 that the nitrogen-RDFs exhibit oscillations and reach a minimum at a distance of 9 Å. These two points are very interesting. We conjecture that the oscillations may be related to the alignment structure of the 5CB. In the chemical structure of 5CB (see figure 1(*d*)), the nitrogen atom lies on the major centrosymmetric axis of the molecule. It is clear in figure 5 that the oscillation shows a periodic variation with a period of 2–4 Å, which is only about half the width of a benzene ring. This indicates that the number of nitrogen atoms in the system changes periodically with the distance from the interface. It can also be seen that the distance from an RDF valley to a peak is about 1 Å, so the alignment structure of 5CB near the fluorinated interface can be hypothesized as follows. (a) The majority of the 5CB molecules are aligned parallel to each other, the nitrogen atoms spaced 2 Å apart. A more possible structure is one in which the biphenyl planes are parallel to each other, which is reasonable because the distance between adjacent nitrogen atoms is around 2 Å and the energy is the lowest in that state. (b) The 1 Å distance of valley to peak indicates that there may be a small number of 5CB molecules that lie between two adjacent biphenyls. In this alignment structure, the distance of nitrogen atoms is about 1 Å; however, the biphenyl distance should be large due to the dense electron cloud between biphenyl structures which would push the inserted molecule out, as outlined in figure 6. This supposition agrees with the pure LC alignment without interfacial interaction [50], which indicates the weaker interfacial effect of the fluorinated interface. The minimum near 9 Å may be related to the cut-off radius which is set as 9.1 Å in the calculations. As mentioned in section 2.1, the interaction between two atoms is very small and will reach zero when the distance is larger than the cut-off radius. Thus, the force between the interface and the nitrogen atoms near 9.1 Å is very weak, and the latter will be pushed away by other closer atoms in the MD process; hence, the number of nitrogen atoms near 9 Å is very small and a minimum of RDF value is observed at this position.

3.6. Orientation behaviour of LCs on the fluorinated interface

The order parameters in the case of weak fluorination (case A) and strong fluorination (case D) are calculated using equation (8). From the results shown in figure 7, a very obvious difference can be found. The change in order parameter in the case of weak fluorination is very small, being in the range of 0.85 ± 0.05. However, in the case of strong fluorination, the range is about 0.55 ± 0.30, the reason for which may be related to the weakening of the interface energy. Such a result has also been observed by Sarkar *et al* in their experiments [16]. They found that the orientation behaviour of LCs becomes disordered with an increasing level of fluorination. Another noticeable point in figure 7 is that the order parameter is 0 when $d < 4.2$ Å, which is approximately the width of the benzene ring. Such a result is quite reasonable from the molecular structure point of view. Moreover, the calculated order parameter in the case of weak fluorination is about 0.85, which

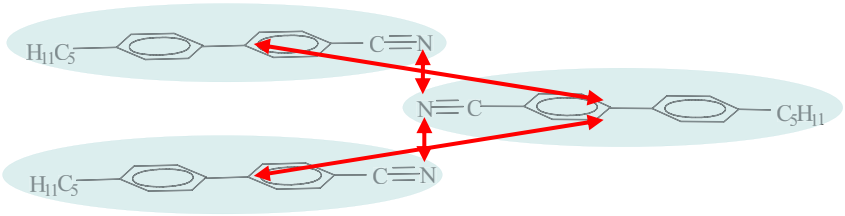

Figure 6. Schematic representation of the 5CB alignment structure near the fluorinated interface. The double-arrows indicate the interaction between the groups.

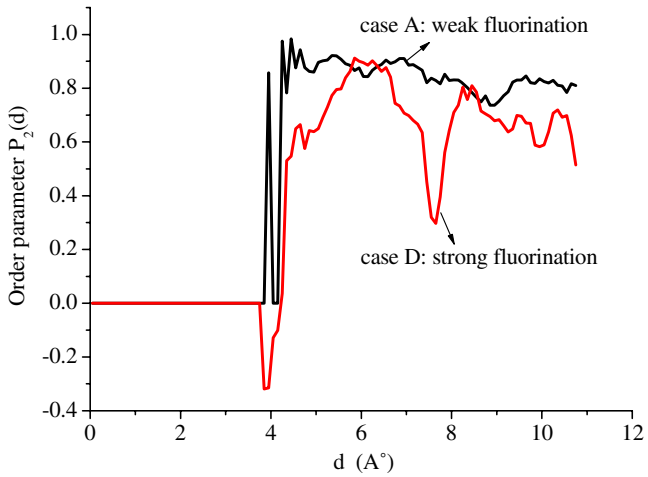

Figure 7. Comparison of orientation behaviour.

is 0.13 larger than the value calculated by Komolkin *et al* [54]. We consider that there may be two reasons for this. (a) The order parameter calculated by Komolkin *et al* is for pure 5CB molecules, that is to say there is no interface effect present. However, in our calculation, there is an interfacial effect even though it is weak. (b) The molecular coordinates used to calculate the order parameter are different.

4. Conclusions

The effects of partial fluorination on interfacial properties have been studied using molecular dynamics methods, focusing on the following aspects: (1) the miscibility and diffusion characteristics of the fluorine-substituted monomer Actyflon; (2) the effects of fluorination level on the distribution of Actyflon near the interface; (3) the interface energy; (4) RDF analysis of nitrogen atoms near the interface; (5) the orientation behaviour of LCs. The most important conclusions are as follows:

(a) Partial fluorination promotes the phase separation of LCs in PIPS. Simultaneously, it can accelerate the diffusion of LCs and monomers as well as lower the photopolymerization rate of monomers, which is helpful in obtaining a better phase separation interface, such as the POLICRYPS structure.

(b) Partial fluorination decreases the interface energy and weakens the interfacial effect of the polymer wall. It is beneficial to decrease the threshold voltage of a PDLC grating. Moreover, the fluorination may be a feasible means for creating the POLICRYPS structure and improving its drive voltage because of the weak interfacial interactions.

(c) Excessive fluorination may lead to penetration of fluorine-substituted monomers into the LC medium, which would block the diffusion of LCs and destroy the grating structure.

(d) Partial fluorination increases the distance between the LC molecules and interface, which may be one of the reasons for the resulting lower interface energy. In addition, the LC alignment structure near the fluorinated interface shows a similar structure to that of pure LCs, which indicates a weak interfacial effect of the fluorinated surface.

(e) Because of the weaker interaction between LCs and the fluorinated interface, the orientation becomes more and more disordered with an increasing level of fluorination.

Using MD methods to investigate complex problems in the fabrication of PDLC gratings is convenient and effective. Moreover, it can provide some valuable insights for improving the performance of PDLC devices.

Acknowledgments

This work was supported by the National Natural Science Foundation of China (Grant Nos 60578035 and 50703039); the State Key Foundation (Grant No 60736042) and the Science Foundation of Jilin Province (Grant Nos 20050520 and 20050321-2).

References

[1] Doane J W, Vaz N A, Wu B G and Zumer S 1986 *Appl. Phys. Lett.* **48** 269
[2] Sutherland R L, Natarajan L V, Tondiglia V P, Bunning T J and Adams W W 1994 *Appl. Phys. Lett.* **64** 1074
[3] Fiske T G, Silverstein L D, Colegrove J and Yuan H 2000 *SID Int. Symp. Dig. Tech. Pap.* **31** 1134
[4] Tanaka K, Kato K and Date M 1999 *Japan. J. Appl. Phys.* **38** L277
[5] Sutherland R L, Natarajan L V, Tondiglia V P and Bunning T J 1993 *Chem. Mater.* **5** 1533
[6] Mucha M 2003 *Prog. Polym. Sci.* **28** 837
[7] Bunning T J, Natarajan L V, Tondglia V P and Sutherland R L 2000 *Ann. Rev. Mater. Sci.* **30** 83
[8] Ostroverkhova O and Moerner W E 2004 *Chem. Rev.* **104** 3267
[9] Liu Y J, Zhang B, Jia Y and Xu K S 2003 *Opt. Commun.* **218** 27

[10] Pogue R T, Sutherland R L, Schmitt M G, Natarajan L V, Siwecki S A, Tondiglia V P and Bunning T J 2000 *Appl. Spectrom.* **54** 1
[11] Vaia R A, Tomlin D W, Schulte M D and Bunning T J 2001 *Polymer* **42** 1055
[12] Klosterman J, Natarajan L V, Tondiglia V P, Sutherland R L, White T J, Guymon C A and Bunning T J 2004 *Polymer* **45** 7213
[13] Jung J A, Kim B K and Kim J C 2006 *Eur. Polym. J.* **42** 2667
[14] Schulte M D, Clarson S J, Natarajan L V, Tomlin D W and Bunning T J 2000 *Liq. Cryst.* **27** 467
[15] Schulte M D, Clarson S J, Natarajan L V, Tomlin D W and Bunning T J 2002 *Mol. Cryst. Liq. Cryst.* **373** 155
[16] Sarkar M D, Qi J and Crawford G P 2002 *Polymer* **43** 7335
[17] McCormick D and Guymon C A 2002 *Mater. Res. Soc. Symp. Proc* **709** CC6.2.1
[18] Hill J R and Sauer J 1994 *J. Phys. Chem.* **98** 1238
[19] Chen C L, Xu W R and Tang L D 2007 *Molecular Simulations* (Beijing: Chemical Industry Press)
[20] Sun H, Mumby S J, Maple J R and Hagler A T 1994 *J. Am. Chem. Soc.* **116** 2978
[21] Sun H 1995 *Macromolecules* **28** 701
[22] Hwang M J, Stockfisch T P and Hagler A T 1994 *J. Am. Chem. Soc.* **116** 2515
[23] Wilson E B, Decius J C and Cross P C 1955 *Molecular Vibrations: The Theory of Infrared and Raman Vibrational Spectra* (New York: Dover)
[24] Maple J A, Hwang M J, Stockfisch T P, Dinur U, Waldman M, Ewig C S and Hagler A T 1994 *J. Comput. Chem.* **15** 162
[25] Maple J R, Thacher T S, Dinur U and Hagler A T 1990 *Chem. Des. Autom. News* **5** 5
[26] Metropolis N, Rosenbluth A W, Rosenbluth M N and Teller A H 1953 *J. Chem. Phys.* **21** 1087
[27] Chen C L, Chen H L, Lee C L and Shih J H 1994 *Macromolecules* **27** 2087
[28] Chen C L, Lee C L, Chen H L and Shih J H 1994 *Macromolecules* **27** 7872
[29] Sen S, Brahma P, Roy S K, Mukherjee D K and Roy S B 1983 *Mol. Cryst. Liq. Cryst.* **100** 327
[30] Press W H, Flannery B P, Teukolsky S A and Vetterling W T 1986 *The Art of Scientific Computing* (Cambridge: Cambridge University Press)
[31] Woodcock L V 1970 *Chem. Phys. Lett.* **10** 257
[32] Swol F V, Woodcock L V and Cape J N 1980 *J. Chem. Phys.* **75** 913
[33] Broughton J Q, Gilmer G H and Weeks J D 1981 *J. Chem. Phys.* **75** 5128
[34] Andersen H C 1980 *J. Chem. Phys.* **72** 2384
[35] Liu Y G, Ma J, Song J, Hu L F and Xuan L 2005 *Chin. J. Liq. Cryst. Disp.* **20** 210
[36] Young D C 2001 *Computational Chemistry* (New York: Wiley)
[37] Hotokkka M 2002 *Molecular Dynamics Simulations* (Cambridge: Cambridge University Press)
[38] Hoover W G 1986 *Molecular Dynamics* (Berlin: Springer)
[39] Stauffer D, Hehl F W, Winkelmann V and Zabolitzky J G 1988 *Computational Physics* (Berlin: Springer)
[40] Yin J H and Mo Z S 2001 *Modern Polymer Physics* (Beijing: Sciences Press)
[41] Rubinstein M and Colby R H 2003 *Polymer Physics* (Oxford: Oxford University Press)
[42] Jung J A and Kim B K 2005 *Opt. Commun.* **247** 125
[43] Adamson A W and Gast A P 1997 *Physical Chemistry of Surface* (New York: Wiley)
[44] Rigby D and Roe R J 1988 *J. Chem. Phys.* **89** 5280
[45] Pasini P, Zannoni C and Zumer S 2003 *Computer Simulation of Liquid Crystal and Polymer* (Dordrecht: Kluwer)
[46] Chalia S R, Wang S Q and Koenig J L 1996 *Appl. Spectrom.* **50** 1339
[47] Veltri A, Caputo R, Umeton C and Sukhov A V 2004 *Appl. Phys. Lett.* **84** 3492
[48] Caputo R, Sio L D, Veltri A, Umeton C and Sukhov A V 2004 *Opt. Lett.* **29** 1261
[49] Caputo R, Sio L D, Veltri A, Umeton C and Sukhov A V 2006 *J. Disp. Tech.* **2** 38
[50] Patnaik S S and Pachter R 1999 *Polymer* **40** 6507
[51] Sutherland R L, Tondiglia V P, Natarajan L V and Bunning T J 2004 *J. Appl. Phys.* **96** 951
[52] Zhang L M, Huang X H and Song X L 2004 *Fundamentals of Materials Science* (Wuhan, China: Wuhan University of Sciences and Technology Press)
[53] Song J, Zheng Z, Liu Y G, Li J and Xuan L 2006 *Chin. J. Liq. Cryst. Display* **21** 443
[54] Komolkin A V and Maliniak A 1995 *Mol. Phys.* **84** 1227